

## **JUTE AND TEA DISCRIMINATION THROUGH FUSION OF SAR AND OPTICAL DATA**

**D. Haldar\***, C. Patnaik, S. Mohan, and M. Chakraborty

Space Applications Centre (ISRO), Ahmedabad, India

**Abstract**—Remote sensing approaches based on both optical and microwave region of EM spectra have been widely adapted for large scale crop monitoring and condition assessment. Visible, infrared and microwave wavelengths are sensitive to different crop characteristics, thus data from optical and radar sensors are complementary. Synthetic Aperture Radar (SAR) responds to the large scale crop structure (size, shape and orientation of leaves, stalks, and fruits) and the dielectric properties of the crop canopy. Research is needed to assess the saturation effects of SAR data and to investigate the synergy between the optical and SAR imagery for exploring various dimensions of crop growth which is not possible with any one of them singly with higher degree of accuracy. An attempt has been made to study the potential of SAR and optical data individually and by fusing them to separate various landcover classes. Two-date and three-date SAR data could distinguish jute and tea crop with 70–85% accuracy, while cloud free optical data (green, red and infrared bands) resulted in accuracy 80–85%. On fusing the optical and SAR single date data of May, 29 2010 using Brovey method, an accuracy of 85% was obtained. PCA and HSV with munsell based approaches resulted in similar accuracies but HSV performed the best among these. This emphasizes on the synergistic effect of SAR and optical data. Also the fused data could be used to delineate the crop condition and age by inputs like NDVI from optical and XPR (Cross polarization ratio) from SAR data.

The co- and cross polarization ratios along with various indices viz. Biomass Index (BMI), Volume Scattering Index (VSI) and canopy structural index (CSI) were used to discriminate tea from jute. Due to differences in structural component of tea and jute at early season as manifested by the indices, there is clear separability as observed from the mean values. Among the dual polarization combinations, HV/VV performed the best (70%) followed by HV/HH (62%) and

---

*Received 30 December 2011, Accepted 19 March 2012, Scheduled 26 March 2012*

\* Corresponding author: Dipanwita Haldar (dipanwita@sac.isro.gov.in).

lastly HH/VV (42%). Among the single best indices for discrimination BMI performed the best. Combination of Co, Cross-polarization and BMI yields around 80% classification accuracy. BMI and VSI combination yielded the best classification accuracy of 84%. This level of accuracy obtained was much superior to that of multivariate HH polarization SAR data.

## 1. INTRODUCTION

Remote sensing primarily uses the spectral, temporal and texture information from remote sensing data to discriminate among different crop types [20]. Few earth observation sensors can provide data with high resolutions in all the spatial, temporal and spectral dimensions, as required for effective identification of crop type.

The ISRO's AWiFS Advanced Wide Field Sensor/LISS 3 Linear Imaging Self Scanner and NASA's Moderate Resolution Imaging Spectroradiometer (MODIS) instrument provide a unique opportunity for monitoring agricultural systems [7]. Data from the above sensors are used in operational mapping of crop type, because they have multiple spectral channels for primary use in land mapping application and also because of its large coverage, high frequency of revisit, small data volume, and low cost compared with higher spatial resolution multispectral satellite data. However, the high spectral and low spatial resolution system has several problems, i.e., mixed pixel problem and number of samples problem, which make it more complicated in crop identification and other types of land cover mapping. The accuracy of a classification process depends mainly on two factors: the sample size and the degree to which the selected sample represents the object of interest [1]. On the other hand, the SAR images from Radarsat-2 provided by the McDonald's Detwiller Associates (MDA) are a good data source for obtaining high resolution spatial information (from 3 m to 100 m depending on the beam mode used) at very high repeat cycle, because of its all-weather and day-night collection capability, low cost, and large coverage (from  $25 \text{ km} \times 25 \text{ km}$  to  $500 \text{ km} \times 500 \text{ km}$  depending on the beam mode). However, radar images are noisy and have no spectral information. Even though field boundaries are recognizable in many beam modes, it is not effective to differentiate crop types just using a single radar image.

Several studies have shown that SAR data may provide information on structural features of the surface complementary to the spectral information in optical data, for instance [3, 4, 15, 17, 18]. It has thus been shown, that the discriminating power of SAR images is very much improved when they are used in combination with optical

data. [17] Have compiled a brief but useful review of multi-source classification. Image fusion is a popular method to integrate different sensors data for obtaining a more suitable image for a variety of applications, such as visual interpretation, image classification, etc.

Various techniques are available for merging multi-sensor image data. Ideally, the merged image should have the following properties [21]: (i) once degraded to the original spatial resolution of the Multispectral (MS) image, the merged image should be as identical as possible to the original MS image; and (ii) the MS set of merged images should be as identical as possible to the MS set that the MS sensor would observe with the high spatial resolution. Methods of merging are often divided into two categories [19]. The first consists of methods which simultaneously take into account all bands in the merging process, whereas the second category groups together those methods which deal separately with the spatial information and each spectral band. The most commonly used methods like intensity-hue-saturation (IHS) and principal component substitution (PCS) belong to the first category. Methods like Brovey, high pass filter (HPF), etc. belongs to the second category. Several authors have used the multi-resolution analysis and wavelet transforms to introduce the spatial information into the spectral bands [6, 12].

The combination of airborne polarimetric SAR with spaceborne SAR and optical data for classification of agricultural land was carried out [5]. Many research papers have reported problems of existing fusion techniques. The most significant problem is color distortion [22]. This problem could lead to poor accuracy in classifying an image, for example, a particular crop type may have a consistent spectral signature in the original, unfused image. However, due to color distortion in the fusion process, the crop type may have several different spectral signatures in the fused image. This means that if the fused image is classified, the crop type may be incorrectly assigned to two or more classification categories. To reduce the color distortion and improve the fusion quality, a wide variety of strategies has been developed, each specific to a particular fusion technique or image set [23]. The rationale to resolve this problem is that image fusion integrates a high resolution SAR image with a low-resolution optical image to produce a high resolution synthetic image, which contains both the high-resolution spatial information of the SAR image and the color information of optical image. The fused image can spatially separate the mixed pixels to a certain degree, resulting in improved the accuracy of classification. The research on image fusion in improving the accuracy of image classification has been reported by at least four authors [2, 8, 11, 16].

## 2. STUDY AREA

The study area selected is northern part of West Bengal covering the District of Jalpaiguri. It is a jute growing area in pre-monsoon season surrounded by tea plantations towards the northern sides and mountainous forests in the extreme north. The crop is sown during first fortnight of April and harvested during second fortnight of August. It is sown mostly with one pre sowing irrigation and well distributed rainfall is required. Upper left bound is  $26^{\circ}51'6.33''\text{N}$ ,  $88^{\circ}11'29.41''\text{E}$  and upper right bound is  $26^{\circ}49'39.33''\text{N}$ ,  $88^{\circ}34'55.33''\text{E}$  and lower left  $26^{\circ}34'10.11''\text{N}$ ,  $88^{\circ}9'43.37''\text{E}$  lower right bound is  $26^{\circ}33'23.78''\text{N}$ ,  $88^{\circ}34'53.27''\text{E}$ .

## 3. DATA USED

Multi-temporal Wide-2 SAR data from Radarsat –2 [C-band, HH/HV-polarization, incidence angle range  $30\text{--}39^{\circ}$  and 2-looks] of May 5 and 29 and June 22, 2010 were used in the study. The Wide 2 data has been selected due to its large area coverage (150-km swath) and reasonable pixel spacing (12.5 m) for crop studies. Acquisition of three sets of SAR data at different crop growth stages were based on the crop calendar. The first date coincided with the initial crop stage, the second date coincided with the peak vegetative stage and the third date was acquired in advanced growth stage. Single date cloud free optical data (LISS 3) of May 29 has been used. Envisat data (May, 08) in IS4 and IS6 beams have been acquired in HV/HH and VV/HH polarizations. The central incidence angle range is 33 to 41 degree and pixel spacing 12.5 m. Ground truth information was collected on all the dates synchronous to satellite pass.

## 4. METHODOLOGY

### 4.1. Ground Truth (GT) Data Collection

The crop is sown during last week of March to mid April. Ground truth data by field survey during the acquisition periods were collected synchronizing with the satellite passes for the area. It included collection of all relevant information on the crop type, stage, height, per cent cover, vigour, soil roughness and moisture status. GPS (Magellan NAVDLX-10) was used during ground truth data collection. Sites having an area greater than 3 hectares occupied by jute or tea were selected for this purpose. In addition ground truth information

pertaining to other land cover like urban, other vegetation, forest, scrub homesteads and water bodies were also collected.

#### 4.2. Satellite Data Processing

Pre-processing of SAR data was carried out using PCI Geomatica ver 9.1 image processing software. The data was downloaded, speckle suppression ( $5 \times 5$  window size), calibration and georeferencing was carried out. The multi-temporal co-registered SAR data was used to identify the crop areas. The ground truth sites were marked on the image and the multi-temporal signatures were analyzed from the mean and standard deviation of the backscatter. From the temporal backscatter values of various ground features, decision rules were formed. The understanding of the interaction of radar with jute/tea crop and the knowledge of plant morphology, cultivation practices and field environment were used during the development of the decision rules. Hierarchical decision rule classification technique was used for the identification of the different land cover classes. After masking out the water, homesteads, urban and fallow areas by the decision rule classification, the vegetation area was then segregated into jute and tea areas based on the temporal backscatter response. Pre-processing of SAR data from ENVISAT ASAR was carried out using both the Basic Envisat SAR Toolbox (BEST) and PCI Geomatica image processing software. The amplitude image was converted to power image, from which the calibration was done to get the backscatter. The dual polarization data was stacked together and filtered. The georeferenced image was used for extraction of the signatures of various crops by studying their backscatter profile in various polarizations.

Atmospheric correction of LISS 3 data was carried out using ATCOR 2. Green, Red and Infrared bands were used for analysis. NDVI has been computed and classification based on single date NDVI range was carried out.

#### 4.3. Fusion of Optical and SAR Data

Before merging, the two datasets were required to be registered to each other. Proper geometric registration is essential to avoid artifacts in the merged image [9]. Twenty control points were selected between Radarsat2 and LISS III data, considering Radarsat2 as the master image. A second-order polynomial equation with an rms error of 0.58 pixel was used to transform the image. The LISS III data were then resampled using the cubic convolution method. The cubic convolution method has been recommended for large changes in pixel size between the original image and the resampled image [13].

The fusion operation using Brovey method was carried out using two optical bands viz Red and Infrared and SAR-HH polarization data. Fusion operation performs data fusion of a Red-Green-Blue colour image or of an input pseudocolour image with a black-and-white intensity image using one of three different fusion models: Cylinder, Hexcone, or Brovey. Cylinder was the original method used by the IHS and RGB programs. The Hexcone model is used by many commercial Image Processing software products. One model can produce more visually pleasing results than the other, depending on the circumstances. The Brovey transform is a highly effective transform that generates a better looking image than the normal RGB image for many types of data, in particular for combining Landsat TM and SPOT Pan imagery and also for optical and SAR data. The Brovey transform is a formula based process that is based on the band to display in a given colour, the sum of all the colour layers, and the intensity layer. Other fusion methods like Principal Component Analysis (PCA), Hue Saturation Value (HSV) transform and HSV based Munsell were performed in ENVI ver 4.2.2.

#### 4.4. Computation of Various Indices

Various indices were computed using single date multi-polarization dataset viz. HH, HV and VV to aid in better classification. The indices were computed from ratios or normalized differences and are largely independent of terrain effects. Various indices apart from the co and cross polarized ratios viz. VSI, CSI, and BMI have been computed to aid in discriminating forest species [10]. We attempted to evaluate these indices for Agricultural crops, to study their feasibility in discriminating crops varying in growth pattern and canopy architecture. The various indices evaluated are summarized below.

**Volume Scattering Index (VSI)** is a measure of the depolarization of the linearly polarized incident radar signal. High values of VSI result when cross polarized backscatter (CS refers to average of cross polarized backscatter) is large with respect to the like polarized average (LK). VSI is an indicator of canopy thickness or density [10].

VSI is computed as

$$\mathbf{VSI} = \mathbf{CS}/(\mathbf{CS} + \mathbf{LK}) \quad (1)$$

where,  $\mathbf{CS} = (\mathbf{HV} + \mathbf{VH})/2$ ,  $\mathbf{LK} = (\mathbf{VV} + \mathbf{HH})/2$  or VSI can be simplified as

$$\mathbf{VSI} = \mathbf{HV}/\{\mathbf{HV} + (\mathbf{VV} + \mathbf{HH})/2\} \quad (2)$$

**Canopy Scattering Index (CSI)** is a measure of the relative importance of vertical versus horizontal structure in vegetation. Ecosystems dominated by nearly vertical trunks or stems will have higher CSI values. Ecosystems with high percentage of double bounce scattering viz. wetlands will have lower CSI than with little double bounce interaction. Thus CSI like other indices is meaningful only when taken in context of interaction type. Canopy scattering is quantified in terms of HV backscatter.

Canopy Structure Index is computed as:

$$\text{CSI} = \text{VV}/(\text{HH} + \text{VV}) \quad (3)$$

The **Biomass Index (BMI)** is an indicator of the relative amount of woody component compared to leafy biomass. BMI is not a ratio and therefore influenced by slope and range effects. BMI is higher for senescent (low fresh leaf biomass) than for evergreen forests due to absorption of microwaves by moist, green younger leaves. This index is best used for vegetated terrain. BMI and VSI respond similarly to biomass changes [10]. The use of BMI does not imply that it is the best measure of biomass, only that biomass is the most relevant biophysical parameter associated with this polarization combination.

Biomass Index is computed as:

$$\text{BMI} = (\text{HH} + \text{VV})/2. \quad (4)$$

The average of the like polarization ratio viz.  $(\text{HH} + \text{VV})/2$  is termed as Biomass Index or LK. The following image sets were investigated: HH, HV and VV polarizations backscatter, Biomass Index ( $\text{BMI} = (\text{HH} + \text{VV})/2$ ), Canopy Structure Index ( $\text{CSI} = \text{VV}/(\text{HH} + \text{VV})$ ) and Volume Scattering Index ( $\text{VSI} = \text{HV}/(\text{HV} + \text{BMI})$ ).

#### 4.5. Data Classification

Single polarization HV, VV and HH were used solely and in the dual pol combinations, HV + VV, HV + HH and HH + VV to study the separability for both Envisat and Radarsat SAR data. Co and Cross-polarization ratios, BMI, VSI and CSI alone and in combination with each other were analysed to study the separability. This separability was not possible with multirate HH polarization data but is possible from HV/HH and HH/VV ratios and derived indices as stated above.

The separability of these two major land covers based on co- and cross-polarization ratios and Biomass index of jute crop/tea plantation is presented in Figs. 1(a) and 1(b). Also the separability based on conjunctive use of the biomass index and volume scattering index with the co and cross polarization ratio has been computed. BMI with co

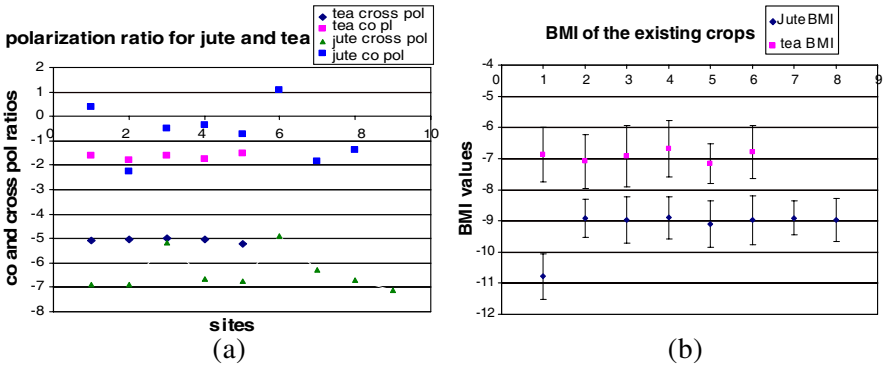


**Figure 1.** Co- and cross-polarization ratios of jute and tea showing the separability Fig. 1(b). Biomass index of jute crop and tea plantation.

and cross polarization ratio shows the best separability as shown in Fig 2(a). The other combinations with lesser separability are shown in Fig. 2(b) to (d).

The optical data singly, two dates SAR and three dates SAR were used for classification. The fused images from PCA, Brovey, HSV, HSV with Munshell were subjected to classification of the major landcovers using maximum likelihood based classification after taking region of interest. Part of ground truth information collected during the field visit was used to train the classifier and part was used to validate the results for accuracy assessment.

## 5. RESULTS AND DISCUSSION DATA CLASSIFICATION AND ACCURACY ASSESSMENT

SAR backscatter from jute and tea crop is governed by various crop and soil parameters during its growth stages and phenological development. Land preparation, sowing, vegetative phase, flowering, fruit formation are the main stages that affect the specific backscatter of cropped areas.

### 5.1. Multitemporal Data Assessment

The temporal variation of the SAR backscatter during crop growth period is examined to decipher the crop phenological information. In addition signature of associated landcover classes was also examined. High backscatter of  $-3$  to  $5$  dB characterized the urban areas and villages in SAR data. These areas appeared bright through out the entire period with very little variation in mean backscatter. Similarly

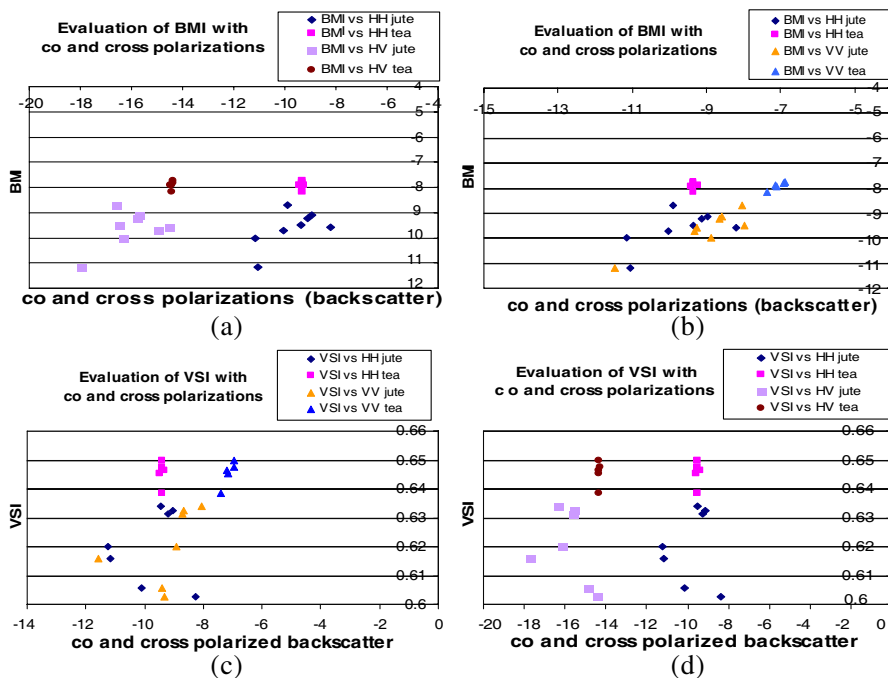


**Figure 2.** (a), (b), (c), (d) BMI vs co and cross polarization and VSI vs co and cross polarization.

very little temporal change in backscatter was observed from forest and homesteads. Low backscatter of less than  $-18$  dB characterized open water bodies like river, ponds and lakes. The non-crop areas such as water, fallow, forest homestead and urban could be delineated from the jute areas based on the evaluation of temporal backscatter.

Backscatter from jute areas has a dynamic range of about 2–3 dB, can be separated from other land cover classes. The signature variation was due to the difference in sowing date, soil moisture and health/density of the crop. The backscatter decreases from first to second date and increased from second to the third date. SAR backscatter as a function of jute age is shown in Fig. 3. The variation is from  $-7$  to  $-9$  dB in the first date,  $-8$  to  $-11$  dB in the second date,  $-5$  to  $-8$  dB in the third date. A consistent dip varying between 1 to 3 dB in the second date was observed for jute. During the third date, canopy was green and maximum numbers of leaves were present (increased number of scatterers) which increased the third date backscatter. Though tea is a perennial crop with distinctly different texture visually but gets mixed up with jute while classifying with

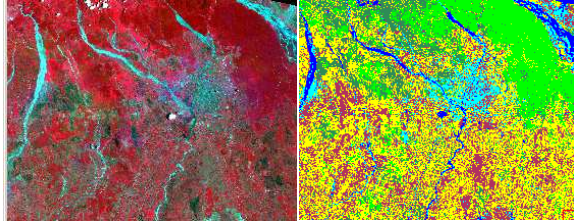


**Figure 3.** FCC image from IR, R and G and corresponding classified image. Green: tea, Yellow: jute, dark green: forests blue: river, cyan: urban, maroon: fallow.

three date temporal profile. Jute is classified with an accuracy of 85% and tea with 80% with overall accuracy of 88% using three date multi-temporal data.

### 5.2. Two Date Single/dual Polarization Assessment Using SAR Data

Classification using Radarsat 2-date HH polarization data (May 5 and May 29) gave an overall accuracy of 78% with an accuracy of 80% for jute, 72% for tea, 64% for fallow. On reducing the datasets to 2-date using HH of May 5 and HH, HV of May 29 classification accuracy of around 86% was observed. The classification accuracy of various landcovers is listed in Table 1. The investigation approves of the fact that dual-pol (HH/HV), 2-date dataset of an appropriate crop stage suffice the classification of the crop cover and is superior to single date SAR datasets. But when optical data adds dimensionality to the SAR data, even a single date data becomes highly multidimensional.

### 5.3. SAR-derived Indices Based Classification

Indices were computed as discussed in the last section. The combination of co, cross pol ratio, VSI, BMI and CSI were used to obtain best possible combination for discrimination of the existing land cover classes. Table 1 summarises the indices based classification accuracy of various crop cover. BMI alone and with other indices gave high accuracy. BMI combined with VSI resulted in 84% overall accuracy. As BMI measures the change in biomass, it is high for forests with woody biomass as compared to leafy evergreen trees [10].

### 5.4. Optical Data Based Classification

The single date optical LISS 3 data of May, 29, 2010 was used for analysis. Jute crop was almost 45 days old and the signature

**Table 1.** Comparative evaluation of various datasets for discrimination of the different landcovers with their classification accuracies.

Data Set	Jute	Tea	Forests	Fallow	Overall accuracy
29th May Optical data (LISS 3) bands IR, R, G	82	86	82	86	80
2-date HH-SAR (5th May and 29th May)	56	80	12	60	54
2-date HH/HV-SAR (5th May and 29th May)	62	82	38	64	70
3-date HH-SAR (5th May, 29th May and 23rd June)	65	80	55	51	62
Co + Crosspol ratio + VSI	60	72	68	63	65
Co + Crosspol ratio + CSI	63	71	70	63	68
Co + Crosspol ratio + BMI	72	78	73	84	80
BMI + CSI	69	74	73	80	75
CSI + VSI	65	70	68	71	68
BMI + VSI	79	81	73	86	84
2 date XPR and 1 date NDVI	78	77	72	95	83
PCA first 3 bands (using 1 dt SAR and 1 dt opt)	71	81	75	76	77
PCA first 3 bands (using 2 dt SAR and 1 dt opt)	94	92	91	95	94
Broye 3 bands	86	79	78	96	85
HSV (Hue Saturation Value) with Munshell	57	96	70	95	84

separability was possible among jute, tea, forested land and fallow using green, red and infrared band of the LISS 3 data. An overall accuracy of 81% with accuracy of 82% for jute, 83% for tea, 80% for forests and 86% for fallow was obtained based on maximum likelihood classification. Fig. 3 shows the FCC and the corresponding classified image. Forests have very high reflectance in IR and high absorption in red band. This difference is less for tea and still lesser for jute. Green reflectance is also higher for forests. Thus these bands aid in appreciably better discrimination.

### 5.5. NDVI and Cross Polarization Ratio (XPR) Based Classification

The XPR is the cross-polarization ratio computed as the ratio of the HH versus HV backscatter. It is a backscatter derivative of both HH and HV term and captures the inherent growth pattern of the canopy. The XPR has been used especially to discriminate the tea plantation from the low vigoured (sparse) forests where the NDVI ranges are in lower bounds and mixes tea plantation with forests. Particularly in these areas red absorption and IR reflectance is less as compared to northern parts. Combined use of cross polarization ratio (XPR) and NDVI in these areas aid in better discrimination. This is also a type of synergy between the SAR and the optical data. In this case an overall accuracy obtained is 83% with accuracy of 79% for jute, 77% for tea, 72% for forests and 95% for fallow was obtained based on maximum likelihood classification. The FCC and the classified image are shown below in Fig. 4.

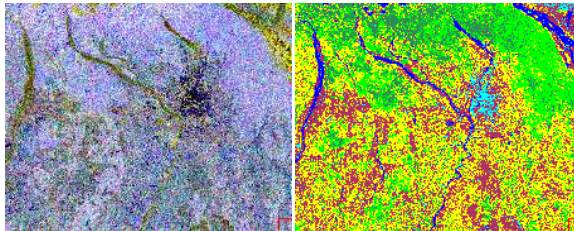


**Figure 4.** FCC from 2 date XPR and 1 date NDVI RGB image of the study area with corresponding classified image.

### 5.6. Fusion Based Classification

The various fusion techniques as described in the methodology has been carried out, the comparison among the various methods are discussed under the following heads.

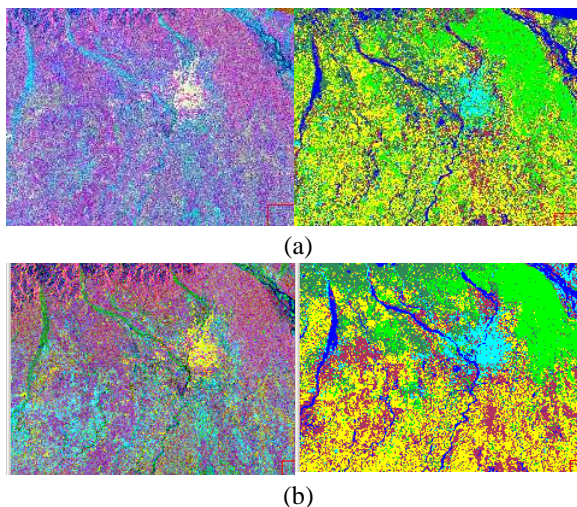


**Figure 5.** FCC from first three principal components with corresponding classified image (a) with 1 date data (b) with 2 date data.

#### 5.6.1. Principal Component Analysis (PCA)

PCA follows a standard methodology of data reduction by orienting the original datasets into a number of orthogonal axes as the number of input bands. The first principal component explains the maximum variability (more than 60% in the present case) followed by second and third. A classification was carried out using the first two, three and four PCs. Principal component analysis was carried out using firstly single date input of three optical bands (green, red and infrared) and same date HH/HV polarization SAR backscatter. An overall accuracy of 77% with accuracy of 71% for jute, 81% for tea, 75% for forests and 76% for fallow was obtained based on maximum likelihood classification. The highest accuracy was obtained with three PCs. Also PCA was carried out with inputs as four optical bands and two date HH/HV SAR backscatter. An overall accuracy of 94% with accuracy of 94% for jute, 92% for tea, 91% for forests and 95% for fallow was obtained based on maximum likelihood classification which was attained using the first three PC. The FCC and classified images are shown in Fig. 5. The confusion among jute and tea in the southern part while using PCs from single date SAR can be overcome by using PCs from both date SAR data. The possible reason is due to the temporal change in volume component of scattering tea and jute rather than single date data where too the pattern is obtained but with lesser accuracy.

### 5.6.2. Brovey Transform

The Brovey Transform attempts to normalize digital number DN values of the multispectral bands and then multiplies the result by the DN of the high spatial resolution data to add the intensity or brightness component of the image [9]. In case of Brovey transformation three input bands were red and infrared from optical data of May 29 and SAR HH polarization backscatter from May 29. The fused image and the classified image is shown in the following figure. An overall accuracy of 85% with accuracy of 86% for jute, 79% for tea, 78% for forests and 96% for fallow was obtained based on maximum likelihood classification. Fig. 6 shows the FCC and classified image of Brovey transform. PCA simply orients the dataset to a new orthogonal plane but Brovey uses a fusion model which synergizes the SAR and optical data where IR, R and optical HH are added synergistically so that the structural component in SAR complements the red absorption and IR reflectance. The results are encouraging as compared to PCA. [14] also reported PCs to be less accurate than Brovey for fused LISS 3 and PAN merged product [14].

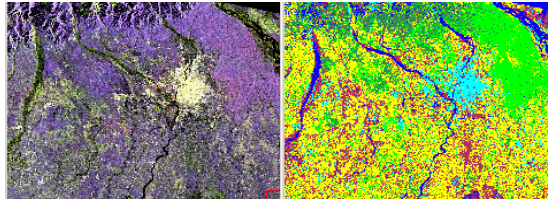


**Figure 6.** FCC from fusion image of optical and SAR data by Brovey transform with corresponding classified image.

### 5.6.3. Hue, Saturation and Value (HSV) Based Fusion

This involves lesser inputs, only three bands, two from optical (red and infrared) and HH polarization backscatter. An overall accuracy of 84% with accuracy of 57% for jute, 96% for tea, 70% for forests and 95% for fallow was obtained based on maximum likelihood classification. In this fusion technique the jute area gets mixed with forests, though it uses the same input bands as the Brovey method, the algorithm is less efficient in synergistically merging the SAR and optical datasets, thus resulting in poor classification accuracy. As pointed out in earlier studies by [22] this poor accuracy is due to colour distortion in case of HSV datasets. Jute has consistent spectral signature in the original datasets but loses it on fusion. The FCC and the classified image are shown below in Fig. 7.

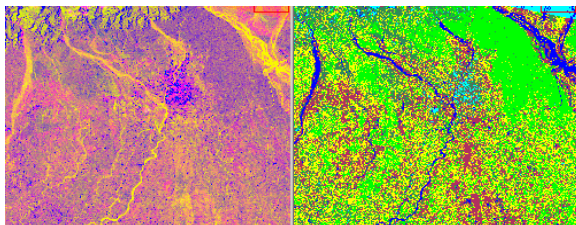


**Figure 7.** FCC from fusion image of optical and SAR data by HSV transform with corresponding classified image.

## 6. CONCLUSION

A comparative evaluation has been carried out to study the potential of optical data for assessing discrimination of pre-monsoon landcover. It has been compared with the assessment of single date and multitemporal SAR data classification. Also fusion results of SAR with optical data for such classification have shown significant improvement over of either SAR or optical data when used singly. Brovey transform has shown highest classification accuracy for single date datasets followed by HSV transform and finally PCs. Though the same inputs have been used for Brovey and HSV, colour distortion has led to poorer accuracy in HSV but Brovey and PCA improve the results of classification. Principal component analysis for single date input performed poorer as compared to the above two. But inputs of two date PC showed significant improvement with 94% overall accuracy. Among the ENVISAT based indices, BMI stands alone as the single best index for discrimination. Combination of Co, Cross-polarization and BMI yields around 80% classification accuracy. BMI and CSI combination yielded the best classification accuracy of 84%. This separability was poor with multirate HH polarization data but is better in HV/HH and HH/VV ratios and derived indices as stated above. The microwave based indices evaluated in this study will be extended to other dominant monsoon and winter landcovers in other areas.

## ACKNOWLEDGMENT

The authors are grateful to Dr. R. R. Navalgund, Director SAC, for his support and guidance. The authors are highly grateful to Dr. J. S. Parihar, Mission Director, EOAM/Deputy Director, EPSA, for his encouragement during the period of investigation.

## REFERENCES

1. Chang, C. I., *Hyperspectral Imaging: Techniques for Spectral Detection and Classification*, Kluwer Academic, New York, 2003.
2. Colditz, R. R., T. Wehrmann, M. Bachmann, K. Steinnocher, M. Schmidt, G. Strunz, and S. Dech, "Influence of imagefusion approaches on classification accuracy — A case study," *International Journal of Remote Sensing*, Vol. 27, No. 15, 3311–3335, 2006.
3. Dobson, M. C., F. T. Ulaby, and L. E. Pierce, "Land-cover classification and estimation of terrain attributes using synthetic aperture radar," *Remote Sensing of Environment*, Vol. 51, 199–214, 1995.
4. Horgan, G. W., C. Glasbey, J. N. Cuevas Gozalo, S. L. Soria, and F. G. Alonso, "Land-use classification in central Spain using SIR-A and MSS imagery," *International Journal of Remote Sensing*, Vol. 13, No. 15, 2839–2848, 1992.
5. Sandholt, I., "The combination of polarimetric SAR with satellite SAR and optical data for classification of agricultural land," *Geografisk Tidsskrift, Danish Journal of Geography*, Vol. 101, 21–32, 1995.
6. Kumar, A. S., B. Kartikeyan, and K. L. Majumder, "Band sharpening of IRS multispectral imagery by cubic spline wavelets," *International Journal of Remote Sensing*, Vol. 21, 581–594, 2000.
7. Lobell, D. B. and G. P. Asner, "Cropland distributions from temporal unmixing of MODIS data," *Remote Sensing of Environment*, Vol. 93, No. 3, 412–422, 2004.
8. Munechika, C. K., J. S. Warnick, C. Salvaggio, and J. R. Schott, "Resolution enhancement of multispectral image data to improve classification accuracy," *Photogrammetric Engineering and Remote Sensing*, Vol. 59, No. 1, 67–72, 1993.
9. Pohl, C. and J. L. Van Genderen, "Multisensor image fusion in remote sensing: Concepts, methods and applications," *International Journal of Remote Sensing*, Vol. 19, 823–854, 1998.
10. Pope, K. O., J. M. Rey-Benayas, and J. F. Paris, "Radar remote sensing of forest and wetland ecosystems in the central american tropics," *Remote Sensing of Environment*, Vol. 48, 205–219, 1994.
11. Prinz, B., R. Wiemker, and H. Spitzer, "Simulation of high resolution satellite imagery from multispectral airborne scanner imagery for accuracy assessment of fusion algorithms," *Proceedings of the ISPRS Joint Workshop 'Sensors and Mapping from Space' of Working Group I/1, I/3 and IV/4*, Hannover,

- Germany, October 1997.
12. Ranchin, T. and L. Wald, "Fusion of high spatial and spectral resolution images: The ARSIS concept and its implementation," *Photogrammetric Engineering and Remote Sensing*, Vol. 66, 49–61, 2000.
  13. Raptis, V. S., R. A. Vaughan, I. N. Hatzopolous, and V. Papapanagiotou, "The use of data fusion for the classification of dense urban environments, the Mytilene case," *Future Trends in Remote Sensing*, Edited by P. Gudmandsen (Rotterdam: Balkema), 427–433, 1998.
  14. Ray, S. S., "Merging of IRS LISS III and PAN data — Evaluation of various methods for a predominantly agricultural area," *Int. J. Remote Sensing*, Vol. 25, No. 13, 2657–2664, July 10, 2004.
  15. Sandholt, I., B. Fog, J. N. Poulsen, M. Stjernholm, and H. Skriver, "Classification of agricultural crops in Denmark using ERS-1 SAR and SPOT imagery," *Sensors and Environmental Applications of Remote Sensing, Proceedings of the 14th EARSeL Symposium*, Askne, J., editor., 37–44, A.A. Balkema Publishers, Rotterdam, Goteborg, Sweden, June 6–8, 1994.
  16. Shaban, M. A. and O. Dikshit, "Evaluation of the merging of SPOT multispectral and panchromatic data for classification of an urban environment," *International Journal of Remote Sensing*, Vol. 23, No. 2, 249–262, 2002.
  17. Solberg, A. H. S., A. K. Jain, and T. Taxt, "Multisource classification of remotely sensed data: Fusion of Landsat TM and SAR images," *IEEE Transactions on Geoscience and Remote Sensing*, Vol. 32, No. 4, 768–785, 1994.
  18. Solberg, A. H. S., T. Taxt, and A. K. Jain, "A markov random field model for classification of multisource satellite imagery," *IEEE Transactions on Geoscience and Remote Sensing*, Vol. 34, No. 1, 100–113, 1996.
  19. Terrettaz, P., "Comparison of different methods to merge SPOT P and XS data: Evaluation in an urban area," *Future Trends in Remote Sensing*, Edited by P. Gudmandsen, 435–443, Rotterdam, Balkema, 1998.
  20. Van Niel, T. G. and T. R. McVicar, "Remote sensing of ricebased irrigated agriculture: A review," *Cooperative Research Centre for Sustainable Rice Production, P1105-01/01*, Yanco, NSW, Australia, 2001.
  21. Wald, L., T. Ranchin, and M. Mangoloni, "Fusion of satellite images of different spatial resolutions: Assessing the quality of resulting images," *Photogrammetric Engineering and Remote*

- Sensing*, Vol. 63, 691–699, 1997.
22. Zhang, Y., “Problems in the fusion of commercial high-resolution satellites images as well as LANDSAT 7 images and initial solutions,” *Proceedings of the ISPRS, CIG, and SDH Joint International Symposium on Geospatial Theory, Processing and Applications*, Ottawa, Canada, unpaginated CD-ROM, July 9–12, 2002.
  23. Zhang, Y., “Understanding image fusion,” *Photogrammetric Engineering and Remote Sensing*, Vol. 66, No. 1, 49–61, 2004.